Biochemical and Biophysical Research Communications 464 (2015) 820–825

Contents lists available at ScienceDirect

Biochemical and Biophysical Research Communications

journal homepage: www.elsevier.com/locate/ybbrc

In vivo photoacoustic imaging of cancer using indocyanine green-labeled monoclonal antibody targeting the epidermal growth factor receptor

Kohei Sano [a, b, 1], Manami Ohashi [a, 1], Kengo Kanazaki [a, c], Ning Ding [a], Jun Deguchi [a], Yuko Kanada [a], Masahiro Ono [a], Hideo Saji [a, *]

[a] Department of Patho-Functional Bioanalysis, Graduate School of Pharmaceutical Sciences, Kyoto University, 46-29 Yoshida Shimoadachi-cho, Sakyo-ku, Kyoto 606-8501, Japan
[b] Kyoto University Hospital, 54 Kawaharacho, Shogoin, Sakyo-ku, Kyoto 606-8507, Japan
[c] Medical Imaging Project, Corporate R&D Headquarters, Canon Inc., 3-30-2 Shimomaruko, Ohta-ku, Tokyo 146-8501, Japan

ARTICLE INFO

Article history:
Received 27 June 2015
Accepted 8 July 2015
Available online 11 July 2015

Keywords:
Photoacoustic imaging
Indocyanine green
Monoclonal antibody
Epidermal growth factor receptor

ABSTRACT

Photoacoustic (PA) imaging is an attractive imaging modality for sensitive and depth imaging of biomolecules with high resolution *in vivo*. The aim of this study was to evaluate the effectiveness of an anti-epidermal growth factor receptor (EGFR) monoclonal antibody (panitumumab; Pan) labeled with indocyanine green derivative (ICG-EG4-Sulfo-OSu), Pan-EG4-ICG, as a PA imaging probe to target cancer-associated EGFR. *In vitro* PA imaging studies demonstrated that Pan-EG4-ICG yielded high EGFR-specific PA signals in EGFR-positive cells. To determine the optimal injection dose and scan timing, we investigated the biodistribution of radiolabeled Pan-EG4-ICG (200–400 μg) in A431 tumor (EGFR++)-bearing mice. The highest tumor accumulation (29.4% injected dose/g) and high tumor-to-blood ratio (2.1) was observed 7 days after injection of Pan-EG4-ICG (400 μg). In *in vivo* PA imaging studies using Pan-EG4-ICG (400 μg), the increase in PA signal (114%) was observed in A431 tumors inoculated in the mammary glands 7 days post-injection. Co-injection of excess Pan resulted in a 35% inhibition of this PA signal, indicating the EGFR-specific accumulation. In conclusion, the ICG-labeled monoclonal antibody (i.e., panitumumab) has the potential to enhance target-specific PA signal, leading to the discrimination of aggressiveness and metastatic potential of tumors and the selection of effective therapeutic strategies.

1. Introduction

Optical imaging is a highly sensitive imaging technique, providing *in vitro* and *in vivo* molecular information in real time without ionizing radiation. Near-infrared (NIR) light, ranging from 650 to 900 nm, enables us to visualize the deeper tissues from the surface, since this wavelength range is relatively penetrative through tissues [1]. However, detection depth (~5 mm) remains the main limitation of the fluorescence imaging method for some applications. On the other hand, photoacoustic (PA) imaging is a new imaging technique with significant promise for biomedical applications. PA imaging detects ultrasonic waves thermoelastically induced by optical absorbers irradiated with pulsed laser [2,3]. Since the ultrasonic waves have much lower tissue scattering, leading to penetration depth of multiple centimeters and sub-millimeter spatial resolution, PA imaging has a potential for a broader clinical translation than other forms of optical imaging.

Recent studies have challenged the clinical cancer diagnosis by PA effect especially for breast cancer [4–6]. Breast cancer was imaged by probing a wide variety of endogenous absorbers such as hemoglobin and melanin in the blood. On the other hand, molecular imaging can be achieved using exogenous PA imaging probes [7]. Some molecular-targeted PA imaging probes based on nanoparticles (i.e., gold nanoparticle) and near-infrared (NIR) fluorescence dyes have been proposed [8–11]. Although nanoparticle-based probes could yield 40–700% increase of PA signal in the tumor [8–10], the biosafety of gold nanoparticles has not been validated, and therefore, these probes have not been applied in a

* Corresponding author. Department of Patho-Functional Bioanalysis, Graduate School of Pharmaceutical Sciences, Kyoto University, 46-29 Yoshida Shimoadachi-machi, Sakyo-ku, Kyoto 606-8501, Japan.
E-mail address: hsaji@pharm.kyoto-u.ac.jp (H. Saji).
[1] These authors contributed equally to this work.

http://dx.doi.org/10.1016/j.bbrc.2015.07.042
0006-291X/

clinical setting yet. Bhattacharyya et al. have reported a NIR fluorescence dye (AlexaFluor750)-conjugated monoclonal antibody against human epidermal growth factor receptor 2 (EGFR2; HER2) as a HER2-targeting PA imaging probe [11]. Although HER2-specific PA signal was demonstrated *in vitro*, *in vivo* data have not yet been reported.

Indocyanine green (ICG) is also a NIR fluorescence dye, which has been approved by the Food and Drug Administration (FDA) and has over 50 years experience of human use [12,13]. ICG is expected to achieve sensitive fluorescence and PA signal, and ICG-labeled probes have been developed for tumor imaging [3,14]. In this study, we selected panitumumab, an FDA-approved monoclonal antibody against human EGFR, as a targeting moiety for molecular imaging of EGFR related to tumor malignancy including cell proliferation, angiogenesis, invasion, and metastasis [15,16]. Thus far, ICG-labeled panitumumab has been reported as an activatable fluorescent probe targeting the EGFR, which yields fluorescence signal only after being bound and processed by the target cancer cells, achieving EGFR-specific fluorescence imaging with high tumor-to-background ratios [17,18]. However, there has been no report of ICG-labeled panitumumab as a PA imaging probe. In this study, the potential of ICG-labeled panitumumab as an EGFR-targeting PA imaging probe was evaluated using mice inoculated with EGFR-positive tumors in the mammary glands.

2. Materials and methods

2.1. Reagents

Panitumumab (Pan) was purchased from Takeda Pharmaceutical Company Ltd. (Osaka, Japan). ICG-EG4-Sulfo-OSu was obtained from Dojindo Molecular Technologies, Inc. (Kumamoto, Japan). *p*-SCN-Bn-DTPA was purchased from Macrocyclics Inc. (Dallas, TX, USA). $^{111}InCl_3$ (74 MBq/mL in 0.02 N HCl) was purchased from Nihon Medi-Physics (Tokyo, Japan). All other chemical used were of the highest purity available.

2.2. Synthesis of Pan-EG4-ICG

According to a previous report [17], ICG-labeling of Pan was performed using ICG with short ethylene glycol linker (ICG-EG4-Sulfo-OSu) to improve the covalent binding of ICG to the antibody. In brief, Pan (0.5 mg, 3.4 nmol) was incubated with ICG-EG4-Sulfo-OSu (32.3 μg, 27.4 nmol) in 0.1 M Na_2HPO_4 (pH8.6) at room temperature (RT) for 1 h, followed by purification with a size exclusion column (PD-10; GE Healthcare UK Ltd., Buckinghamshire, UK). The concentration of ICG and antibody was determined by measuring the absorption at 768 nm and 280 nm with a UV–Vis NIR system (UV-1800, Shimadzu Co., Kyoto, Japan) to determine the number of ICG molecules conjugated with each antibody molecule.

2.3. Measurement of PA signal in vitro

The measurement of PA signal of Pan-EG4-ICG solution was performed according to the method reported previously [14] with a slight modification. Pulsed light with a wavelength of 810 nm generated by the Model Titanium Sapphire Laser system was used. Pan-EG4-ICG (final concentration: 0, 66, 132, and 264 μg/mL) was incubated in phosphate buffered saline (PBS) or in 1% sodium dodecyl sulfate (SDS)/PBS for 20 min at RT. The PA signal of Pan-EG4-ICG solution was measured as mentioned above.

2.4. Cell culture

The cell lines highly expressing EGFR (A431 and MDA-MB-468) and the low EGFR expressing cell line, T47D [19,20], were provided by RIKEN BRC through the National Bio-Resource Project of the MEXT, Japan. The EGFR-positive cell lines were grown in Roswell Park Memorial Institute medium (RPMI) 1640 (Life Technologies Co., Carlsbad, CA, USA) containing 10% fetal bovine serum, 0.03% L-glutamine, 100 units/mL penicillin, and 100 μg/mL streptomycin in 5% CO_2 at 37 °C. T47D cells were grown in Dulbecco's Modified Eagle's medium (DMEM) containing 10% fetal bovine serum, 100 units/mL penicillin, and 100 μg/mL streptomycin in 5% CO_2 at 37 °C.

2.5. In vitro PA imaging studies

In vitro PA imaging was performed to evaluate the cellular uptake of Pan-EG4-ICG. Each cell line was plated and left to grow on a 25 cm^2 flask for 2 days. Pan-EG4-ICG (10 μg/mL) was added to the flask. After 6 h of incubation, the cells were washed with PBS and collected into tubes. PA images of cell pellets (1×10^6 cells) were acquired by Nexus 128 instrument (Endra Inc., Ann Arbor, MI, USA) under the conditions of 20 angles and 120 pulses per angle as reported previously [14]. The excitation wavelength of pulse laser was 808 nm. After reconstruction of PA images *via* Osirix software, PA signal intensity was analyzed by AMIDE after normalization with irradiated laser intensity. To validate the specific binding of Pan-EG4-ICG, excess antibody (100 μg/mL) was used for blocking studies.

2.6. Tumor model

The animal experiments were performed according to institutional guidelines and approved by the Kyoto University Animal Care Committee. All surgery was performed under isoflurane anesthesia, and all efforts were made to minimize suffering. BALB/c-nu/nu nude mice (five-week-old, female) were purchased from Japan SLC Inc. (Hamamatsu, Japan). The animals were housed under a 12-h light/dark cycle and allowed free access to food (D10001, Japan SLC, Inc.) and water. A431 cells (2×10^6) suspended in 50 μL PBS were injected subcutaneously into the left abdominal mammary glands of the mice. The experiments were conducted when tumors grew to about 7–8 mm 14 days after inoculation.

2.7. Biodistribution studies

In order to determine the optimal injection dose and scan timing for PA imaging after injection of Pan-EG4-ICG, the biodistribution study of ^{111}In-labeled Pan-EG4-ICG was performed. ^{111}In-labeled Pan-EG4-ICG was synthesized as described below. *p*-SCN-Bn-DTPA dissolved in phosphate buffer (0.1 M, pH 8.6) was mixed with Pan-EG4-ICG at a molar ratio of 20:1, followed by incubation for 6 h at 37 °C under protection from light. After purification with a diafiltration membrane (Amicon Ultra Centrifugal Filter Unit (nominal molecular weight limit of 30 kDa), Millipore Co., Darmstadt, Germany) with 0.1 M acetate buffer (pH 6.0), DTPA-Pan-EG4-ICG was obtained. The number of DTPAs conjugated to Pan-EG4-ICG was approximately 0.5. ^{111}In-labeling was performed by mixing of DTPA-Pan-EG4-ICG with $^{111}InCl_3$ in acetate buffer followed by incubation for 15 min at RT. Before injection into mice, the buffer exchange was performed by a diafiltration membrane with PBS. Radiochemical purity, calculated using PD-10 columns (GE Healthcare UK Ltd.), was more than 99%. The mixture of ^{111}In-DTPA-Pan-EG4-ICG and Pan-EG4-ICG (200, 300, or 400 μg, 37 kBq/mouse) was administered into A431 tumor bearing mice intravenously and the biodistribution was evaluated at 2, 3, 5, and 7 days

after injection (n = 3 for each time point). Organs of interest including tumors were excised. The organ weights were determined, and the radioactivity in the organs was measured with a NaI well-type scintillation counter (1470WIZARD, PerkinElmer Inc. Waltham, MA, USA). Data were calculated as the percentage of injected dose per gram of tissue (%ID/g).

2.8. In vivo PA imaging studies

A431 tumor bearing mice received an intravenous injection of Pan-EG4-ICG (400 μg). Before and 7 days after administration, mice were imaged with a Nexus 128 instrument (808 nm, 120 angles, 100 pulses per angle) under isoflurane anesthesia (n = 3). To validate the EGFR-specific accumulation of the Pan-EG4-ICG in the tumor, excess panitumumab (2 mg) was co-injected for blocking studies (n = 3). After reconstruction of PA images *via* Osirix software, PA signal intensity was analyzed by AMIDE after normalization with irradiated laser intensity.

2.9. Depth information by PA imaging and fluorescence imaging technique

The intralipid gel (1-cm-thick) of 1% intralipid was prepared as previously reported [14] because it is considered as a scattering substance of a living body [21]. Tumors (n = 6) were excised from A431 tumor-bearing mice injected with Pan-EG4-ICG (400 μg), and *ex vivo* fluorescence and PA imaging of tumors was conducted with or without coverage of intralipid gel. The apparent tumor size was calculated based on half-value width of the maximum signal intensity.

2.10. Statistical analysis

Quantitative data were expressed as mean ± SD. Means were compared using two-way factorial ANOVA followed by the Tukey–Kramer test. *P*-values <0.05 were considered statistically significant.

3. Results

3.1. Synthesis of Pan-EG4-ICG

The number of ICG molecules conjugated to a Pan molecule was 2.6 ± 0.2. SDS-polyacrylamide gel electrophoresis (PAGE) confirmed that more than 87% of ICG was covalently bound to Pan (Supplementary Fig. 1), which was consistent with a previous report [17].

3.2. Phantom imaging studies

PA signal of Pan-EG4-ICG in PBS or SDS/PBS increased proportionally to ICG concentration and SDS treatment increased it by about 2-fold. This was determined based on the absorbance difference at 810 nm with or without SDS treatment (Fig. 1A, B). On the other hand, *in vitro* fluorescence phantom imaging of Pan-EG4-ICG solution demonstrated that the dilution with PBS showed little fluorescence signal in the concentration range of 0–200 μg/mL, while SDS treatment induced fluorescence dequenching, leading to about 10-fold increase of ICG fluorescence signal intensity compared to that by the control solution (Supplementary Fig. 2A, B), as reported previously [17].

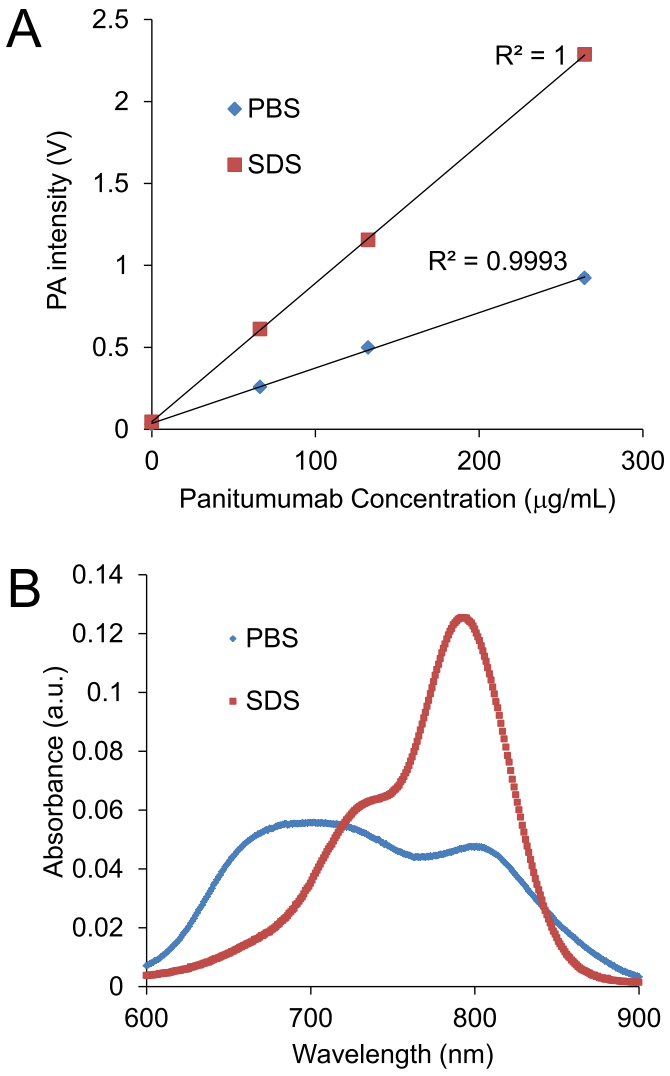

Fig. 1. Photoacoustic properties of Pan-EG4-ICG. (A) PA signal intensities of Pan-EG4-ICG in PBS or 1% SDS/PBS. (B) Absorption spectra of Pan-EG4-ICG in PBS or 1% SDS/PBS. NIR absorbance spectrum was changed, and an approximately two-fold increase of absorbance at 810 nm was observed by mixing with 1% SDS.

3.3. In vitro PA imaging studies

The cellular uptake of Pan-EG4-ICG was evaluated by *in vitro* PA imaging (Fig. 2A, B). The marked increase of PA signals was observed in EGFR-positive A431 and MDA-MB-468 cells 6 h after incubation (109% and 62% increase in A431 and MDA-MB-468 cells, respectively, when compared with control cells), which was significantly decreased by co-treatment with an excess of Pan (33% and 32% decrease in A431 and MDA-MB-468 cells, respectively, when compared to the 6 h incubation group), suggesting the EGFR-specific binding. In the EGFR-negative T47D cells, only a little increase of PA signal was detected at 6 h after incubation.

3.4. Biodistribution studies

Results of *in vivo* biodistribution studies of ^{111}In-labeled Pan-EG4-ICG (200, 300, and 400 μg) are summarized in Table 1. The high level of accumulation (%ID/g tissue) of Pan-EG4-ICG in the tumor was retained at each time point (24.4, 24.9, and 29.4%ID/g for 200, 300, and 400 μg group, respectively at 7 days post-injection)

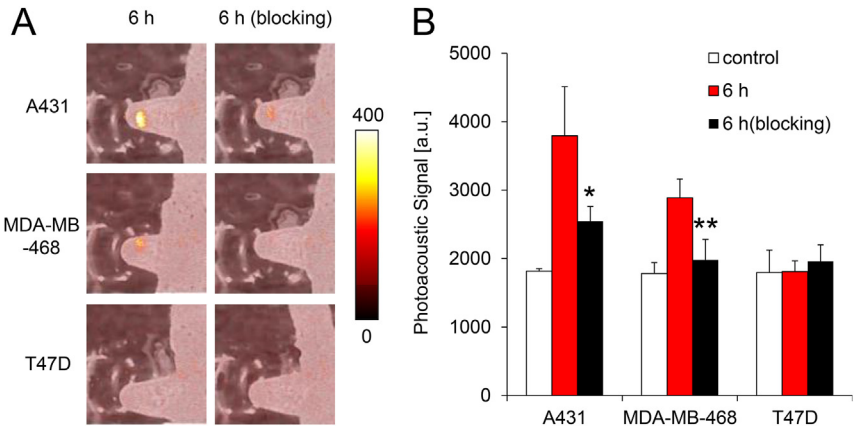

Fig. 2. *In vitro* cellular binding assay with Pan-EG4-ICG. (A) *In vitro* PA images of A431, MDA-MB-468, and T47D cells after incubation with Pan-EG4-ICG for 6 h. The cell pellets are at the tips of tubes after centrifugation. Excess Pan (100 μg/mL) was added 1 h before incubation with Pan-EG4-ICG for blocking studies. (B) PA signal intensity (a.u.) calculated from *in vitro* PA images of Pan-EG4-ICG. $^{*}P < 0.05$, $^{**}P < 0.01$.

independently of the injected dose. The *in vivo* PA signal in the tumor can be dependent on the products of injected ICG molecules multiplied by probe accumulation (%ID/g tissue) in the tumor. Therefore, Pan-EG4-ICG (400 μg; maximum injected dose used) at day 7 post-injection (highest accumulation in the tumor, 29.4%ID/g) should exhibit the highest PA signal intensity in the tumor. The tumor-to-background ratio is also an essential factor to achieve a high-contrast tumor imaging. The tumor-to-blood (T/B) and tumor-

Table 1
Biodistribution results of ^{111}In-DTPA-Pan-EG4-ICG (200, 300, and 400 μg/mouse) in A431 tumor bearing nude mice. Results are expressed as means (%ID/g) ± SD (n = 3 for each group).

Organs	Day 2	Day 3	Day 5	Day 7
^{111}In-DTPA-Pan-EG4-ICG 200 μg				
Blood	21.91 ± 2.13	19.48 ± 3.46	17.84 ± 1.45	13.30 ± 0.75
Heart	4.62 ± 0.43	4.16 ± 0.43	2.87 ± 0.36	2.77 ± 0.05
Lungs	7.0 4 ± 1.35	5.94 ± 0.82	5.46 ± 1.26	3.89 ± 0.48
Liver	10.99 ± 2.67	9.42 ± 0.35	8.18 ± 0.53	5.42 ± 0.41
Kidneys	5.67 ± 0.61	4.04 ± 0.35	3.92 ± 0.44	2.85 ± 0.08
Stomach	1.27 ± 0.35	1.03 ± 0.19	1.13 ± 0.27	0.75 ± 0.35
Intestine	1.13 ± 0.07	0.98 ± 0.08	1.19 ± 0.14	0.92 ± 0.12
Pancreas	1.67 ± 0.12	1.34 ± 0.25	1.74 ± 0.04	1.61 ± 0.40
Spleen	7.80 ± 1.18	4.88 ± 0.42	5.01 ± 0.56	3.52 ± 0.16
Muscle	1.18 ± 0.46	1.14 ± 0.48	1.98 ± 0.22	2.28 ± 1.09
A431 tumor	23.95 ± 3.10	25.90 ± 2.91	25.29 ± 3.77	24.35 ± 1.42
Tumor/blood ratio	1.09 ± 0.08	1.34 ± 0.15	1.42 ± 0.16	1.83 ± 0.06
Tumor/muscle ratio	22.78 ± 10.50	24.73 ± 8.16	12.85 ± 2.27	11.97 ± 4.07
^{111}In-DTPA-Pan-EG4-ICG 300 μg				
Blood	24.40 ± 3.00	19.22 ± 3.97	16.73 ± 2.05	11.22 ± 1.79
Heart	5.36 ± 1.30	4.10 ± 0.46	3.32 ± 0.78	3.10 ± 0.65
Lungs	8.80 ± 0.61	7.11 ± 0.88	6.12 ± 1.09	4.02 ± 0.86
Liver	11.50 ± 0.93	9.19 ± 0.45	8.32 ± 1.45	6.14 ± 1.45
Kidneys	5.58 ± 0.83	4.07 ± 0.66	4.17 ± 0.88	3.05 ± 0.50
Stomach	0.94 ± 0.24	0.93 ± 0.22	1.50 ± 0.42	0.96 ± 0.34
Intestine	1.25 ± 0.12	0.94 ± 0.15	1.30 ± 0.20	0.95 ± 0.26
Pancreas	1.80 ± 0.50	1.42 ± 0.25	1.94 ± 0.34	1.46 ± 0.23
Spleen	7.08 ± 1.19	5.11 ± 0.80	5.22 ± 0.65	3.70 ± 1.26
Muscle	1.34 ± 0.35	1.04 ± 0.14	1.95 ± 0.25	2.90 ± 0.30
A431 tumor	20.11 ± 2.33	20.81 ± 3.67	24.33 ± 2.62	24.89 ± 2.29
Tumor/blood ratio	0.83 ± 0.13	1.09 ± 0.07	1.46 ± 0.06	2.23 ± 0.16
Tumor/muscle ratio	16.04 ± 6.49	19.96 ± 1.34	12.66 ± 2.47	12.13 ± 6.71
^{111}In-DTPA-Pan-EG4-ICG 400 μg				
Blood	20.47 ± 1.96	16.37 ± 2.37	15.90 ± 1.49	14.25 ± 1.29
Heart	3.44 ± 0.56	3.05 ± 0.67	3.25 ± 0.11	3.10 ± 0.35
Lungs	6.50 ± 0.36	4.87 ± 0.45	5.17 ± 0.20	4.67 ± 0.06
Liver	12.11 ± 1.50	11.09 ± 3.13	7.19 ± 0.28	5.42 ± 0.26
Kidneys	3.95 ± 0.27	3.98 ± 0.29	4.25 ± 0.64	3.81 ± 0.46
Stomach	1.11 ± 0.47	1.28 ± 0.36	1.56 ± 0.44	0.76 ± 0.31
Intestine	1.28 ± 0.15	1.42 ± 0.22	1.23 ± 0.16	0.99 ± 0.14
Pancreas	1.69 ± 0.25	1.53 ± 0.30	1.74 ± 0.13	1.42 ± 0.23
Spleen	5.23 ± 0.41	4.44 ± 0.46	3.90 ± 0.50	3.71 ± 0.10
Muscle	1.68 ± 0.08	1.72 ± 0.39	1.86 ± 0.15	1.66 ± 0.24
A431 tumor	16.85 ± 2.07	16.16 ± 3.27	23.53 ± 2.18	29.35 ± 0.95
Tumor/blood ratio	0.83 ± 0.12	0.98 ± 0.07	1.48 ± 0.04	2.07 ± 0.24
Tumor/muscle ratio	10.08 ± 1.73	9.49 ± 1.23	12.78 ± 2.12	17.98 ± 3.00

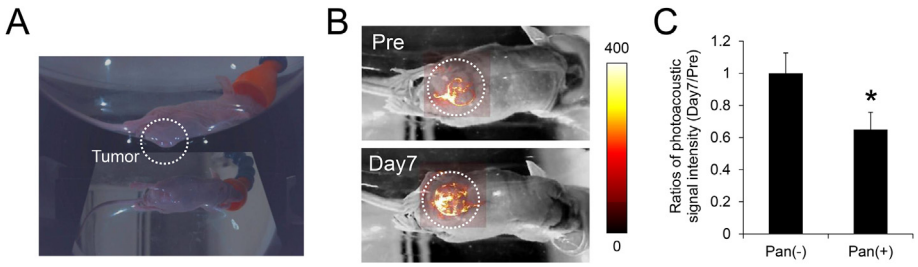

Fig. 3. *In vivo* PA imaging. (A) Placement of the mouse in bowl. The measurement region was indicated by the circle drawn by the dashed line. (B) PA images were acquired before and 7 days after injection of Pan-EG4-ICG (400 μg). The circles drawn by the dashed line represent the tumor regions. (C) PA signal intensity ratios (24 h post-injection/pre-injection) calculated from PA images (B). For blocking studies, excess Pan was co-injected with Pan-EG4-ICG. Values are represented as mean ± SD. n = 3.

to-muscle (T/M) ratios increased with time and reached 2.1 and 18.0, respectively, 7 days after injection of Pan-EG4-ICG (400 μg).

3.5. *In vivo* PA imaging studies

Based on the results of the *in vivo* biodistribution study using ^{111}In-labeled Pan-EG4-ICG, the photoacoustic images of A431 tumor bearing mice intravenously injected with 400 μg of Pan-EG4-ICG were acquired 7 days post-injection (Fig. 3A, B). A 114% increase in PA signal was observed in the tumor compared to pre-injection (Fig. 3B). PA signals in the tumors were significantly blocked (35% decrease of PA signals) by co-treatment with an excess of unconjugated Pan (Fig. 3C), demonstrating that PA signals partly derived from the Pan-EG4-ICG bound to EGFR expressed in the tumor cells.

3.6. *Depth information by PA imaging and fluorescence imaging technique*

By coverage of tumors with intralipid gel, the marked decrease of fluorescence signal intensity (70.2%) and the increase of fluorescence signal area (2.5-fold) were observed (Fig. 4A, C), whereas PA signal area did not change regardless of intralipid coverage, although the PA signal intensity decreased in part (52%) (Fig. 4B, C). As shown in our previous study using ICG-labeled human serum albumin [14], the PA signal intensity was significantly higher than fluorescence signal intensity in the presence of intralipid gel ($P < 0.01$, Fig. 4C), while the apparent tumor size in fluorescence imaging was significantly larger than that in PA imaging ($P < 0.01$, Fig. 4C).

4. Discussion

Optical imaging has many theoretical advantages for tumor identification and characterization. The on-off switching of fluorescence signal is one approach to reduce the background signal by utilizing the activation mechanism. The fluorescence can be quenched or activated depending on its chemical state. The ICG-labeled monoclonal antibodies were proposed as activatable molecular imaging probes. This approach can provide a high tumor-to-background ratio as shown in Supplementary Figure 3 and previous studies [17,18]. However, detection depth (~5 mm) remains the main limitation of the fluorescence imaging method for some applications [2] as shown in Fig. 4. On the other hand, it was confirmed that PA imaging has the potential to detect tumors with a high sensitivity and resolution because of its ultrasonic characteristics (Fig. 4).

To date, some attempts to develop PA probes for molecular imaging have been reported [8–11,22]. An ICG-labeled single walled nanotube (SWNT) has been proposed as a tumor-targeting PA probe. The ICG-SWNT conjugates yielded an intense increase of PA signal (200%) and tumor-to-background ratios [22]. However, the clinical study has not been conducted yet because of its long-term toxicity (aggregation) in the liver, lung, and spleen [23]. Gold nanorods also produced target-specific PA signals. However, the biocompatibility in humans remains controversial. On the other hand, as a PA probe based on a monoclonal antibody, the anti-HER2 monoclonal antibody conjugated with the AlexaFluor750 dye exhibited a HER2-specific PA signal *in vitro* [11]. In this study, we selected ICG as a PA signal emitter because ICG has a longer Ex/Em wavelength (Ex/Em = 774/805 nm) than AlexaFluor750 (Ex/Em = 753/782 nm), which allows photons to penetrate biological

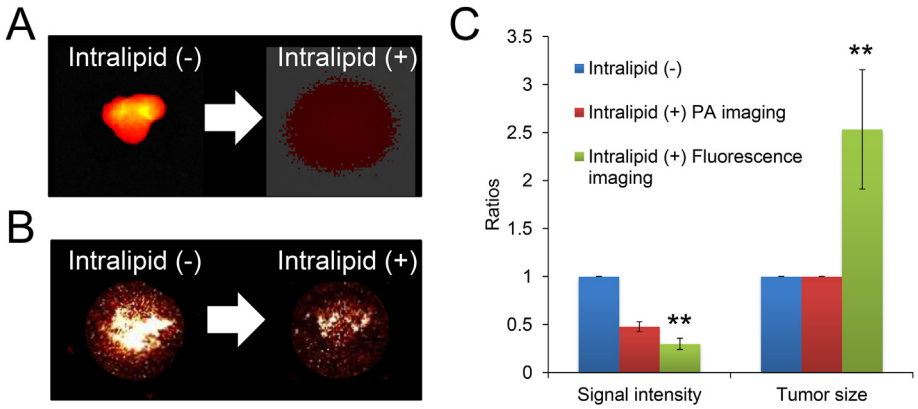

Fig. 4. Depth information by fluorescence and PA imaging. Fluorescence images (A) and PA images (B) of the tumor injected with Pan-EG4-ICG with (right) and without (left) intralipid gel. (C) Changes in the ratios of signal intensity and tumor size in the PA and fluorescence imaging with and without intralipid gel. $^{**}P < 0.01$.

tissues with relatively high transmittance, enabling depth molecular imaging. Furthermore, quantum yield of ICG is 10-time lower than that of AlexaFluor750, which could enhance the production of thermal energy and ultrasonic waves, although the molar extinction coefficient of ICG (147,000 cm^{-1} M^{-1}) is two-fold lower compared to that of AlexaFluor750 (290,000 cm^{-1} M^{-1}). Pan-EG4-ICG enhanced PA signal by 114% at 7 days post-injection and allowed a clear visualization of EGFR-positive tumors inoculated in the mammary glands in our breast cancer mouse model (Fig. 3B). A slight PA signal was observed before probe injection, which was derived from hemoglobin in the blood. Because both ICG and Pan were FDA-approved, each component would have a favorable toxicity profile, although formal toxicity studies of Pan-EG4-ICG will be required.

The injected dose of Pan-EG4-ICG used in this study (400 μg/mouse [20 g]) was approximately 2–3-fold higher compared to the therapeutic dose (maximum therapeutic dose 12 mg/kg). To used in a clinical trial, the injected dose should be decreased. As the number of ICG molecules conjugated to Pan increased, the accumulation of Pan-EG4-ICG in the liver was markedly increased due to the liver targeting of ICG [24], resulting in a decrease in tumor accumulation (Supplementary Fig. 4). Therefore, because it is essential to improve the sensitivity for safe use of probes in clinical settings, the drug design (using a biocompatible drug carrier or slight modification of ICG molecule) or improvement of detector sensitivity would be required. In conclusion, ICG-labeled monoclonal antibody (i.e., panitumumab) has the potential to enhance target-specific PA signal, leading to the discrimination of aggressiveness and metastatic potential of tumors and the selection of effective therapeutic strategies. However, the injected dose should be improved before its application in clinical trials.

Acknowledgments

This work was supported by the Innovative Techno-Hub for Integrated Medical Bio-imaging Project of the Specific Coordination Funds for Promoting Science and Technology, from the Ministry of Education, Culture, Sports, Science and Technology (MEXT), Japan. Part of this study was supported by JSPS KAKENHI Grant Number 15H04637.

Appendix A. Supplementary data

Supplementary data related to this article can be found at http://dx.doi.org/10.1016/j.bbrc.2015.07.042.

Transparency document

Transparency document related to this article can be found online at http://dx.doi.org/10.1016/j.bbrc.2015.07.042.

References

[1] H. Kobayashi, M. Ogawa, R. Alford, et al., New strategies for fluorescent probe design in medical diagnostic imaging, Chem. Rev. 110 (2010) 2620–2640.
[2] S. Mallidi, G.P. Luke, S. Emelianov, Photoacoustic imaging in cancer detection, diagnosis, and treatment guidance, Trend Biotechnol. 29 (2011) 213–221.
[3] A. de la Zerda, S. Bodapati, R. Teed, et al., Family of enhanced photoacoustic imaging agents for high-sensitivity and multiplexing studies in living mice, ACS Nano 6 (2012) 4694–4701.
[4] M. Heijblom, D. Piras, W. Xia, et al., Visualizing breast cancer using the Twente photoacoustic mammoscope: what do we learn from twelve new patient measurements? Opt. Express 20 (2012) 11582–11597.
[5] T. Kitai, M. Torii, T. Sugie, et al., Photoacoustic mammography: initial clinical results, Breast Cancer Tokyo Jpn. 21 (2014) 146–153.
[6] S. Manohar, S.E. Vaartjes, J.C. van Hespen, et al., Initial results of in vivo non-invasive cancer imaging in the human breast using near-infrared photoacoustics, Opt. Express 15 (2007) 12277–12285.
[7] G.P. Luke, D. Yeager, S.Y. Emelianov, Biomedical applications of photoacoustic imaging with exogenous contrast agents, Ann. Biomed. Eng. 40 (2012) 422–437.
[8] P.C. Li, C.R. Wang, D.B. Shieh, et al., In vivo photoacoustic molecular imaging with simultaneous multiple selective targeting using antibody-conjugated gold nanorods, Opt. Express 16 (2008) 18605–18615.
[9] K. Cheng, S.R. Kothapalli, H. Liu, et al., Construction and validation of nano gold tripods for molecular imaging of living subjects, J. Am. Chem. Soc. 136 (2014) 3560–3571.
[10] Y. Xia, W. Li, C.M. Cobley, et al., Gold nanocages: from synthesis to theranostic applications, Acc. Chem. Res. 44 (2011) 914–924.
[11] S. Bhattacharyya, S. Wang, D. Reinecke, et al., Synthesis and evaluation of near-infrared (NIR) dye-herceptin conjugates as photoacoustic computed tomography (PCT) probes for HER2 expression in breast cancer, Bioconjugate Chem. 19 (2008) 1186–1193.
[12] S.G. Sakka, Assessing liver function, Curr. Opin. Crit. Care 13 (2007) 207–214.
[13] V.L. Dzurinko, A.S. Gurwood, J.R. Price, Intravenous and indocyanine green angiography, Optometry 75 (2004) 743–755.
[14] K. Kanazaki, K. Sano, A. Makino, et al., Development of human serum albumin conjugated with near-infrared dye for photoacoustic tumor imaging, J. Biomed. Opt. 19 (2014) 96002.
[15] W.J. Gullick, J.J. Marsden, N. Whittle, et al., Expression of epidermal growth factor receptors on human cervical, ovarian, and vulval carcinomas, Cancer Res. 46 (1986) 285–292.
[16] D.S. Salomon, R. Brandt, F. Ciardiello, et al., Epidermal growth factor-related peptides and their receptors in human malignancies, Crit. Rev. Oncol. Hematol. 19 (1995) 183–232.
[17] K. Sano, T. Nakajima, K. Miyazaki, et al., Short PEG-linkers improve the performance of targeted, activatable monoclonal antibody-indocyanine green optical imaging probes, Bioconjugate Chem. 24 (2013) 811–816.
[18] M. Ogawa, N. Kosaka, P.L. Choyke, et al., In vivo molecular imaging of cancer with a quenching near-infrared fluorescent probe using conjugates of monoclonal antibodies and indocyanine green, Cancer Res. 69 (2009) 1268–1272.
[19] J. Anido, P. Matar, J. Albanell, et al., ZD1839, a specific epidermal growth factor receptor (EGFR) tyrosine kinase inhibitor, induces the formation of inactive EGFR/HER2 and EGFR/HER3 heterodimers and prevents heregulin signaling in HER2-overexpressing breast cancer cells, Clin. Cancer Res. 9 (2003) 1274–1283.
[20] J. Howlin, J. Rosenkvist, T. Andersson, TNK2 preserves epidermal growth factor receptor expression on the cell surface and enhances migration and invasion of human breast cancer cells, Breast Cancer Res. 10 (2008) R36.
[21] J.R. Cook, R.R. Bouchard, S.Y. Emelianov, Tissue-mimicking phantoms for photoacoustic and ultrasonic imaging, Biomed. Opt. Express 2 (2011) 3193–3206.
[22] A. de la Zerda, Z. Liu, S. Bodapati, et al., Ultrahigh sensitivity carbon nanotube agents for photoacoustic molecular imaging in living mice, Nano Lett. 10 (2010) 2168–2172.
[23] S.T. Yang, X. Wang, G. Jia, et al., Long-term accumulation and low toxicity of single-walled carbon nanotubes in intravenously exposed mice, Toxicol. Lett. 181 (2008) 182–189.
[24] G.R. Cherrick, S.W. Stein, C.M. Leevy, et al., Indocyanine green: observations on its physical properties, plasma decay, and hepatic extraction, J. Clin. Invest. 39 (1960) 592–600.